International Journal of Geosciences, 2026, 17(9), 636-651
https://www.scirp.org/journal/ijg
ISSN Online: 2156-8367
ISSN Print: 2156-8359

Application of Geospatial Tools and Hierarchical Multi-Criteria Analysis to the Study of Coastal Vulnerability to Flooding in San Pedro (South-West of the Ivory Coast)

Anzoumanan Kamagate[1], **Attoungbre Jean-Philippe Deguy**[2], **Seydou Diallo**[2]

[1]Training and Research Unit for Marine Sciences, University of San-Pedro, San-Pedro, Côte d'Ivoire
[2]Geosciences and Environment Laboratory (LGE), Training and Research Unit for Environmental Sciences and Management, University Nangui Abrogoua (UNA), Abidjan, Côte d'Ivoire
Email: anzoumanan.kamagate@usp.edu.ci

How to cite this paper: Kamagate, A., Deguy, A.J.-P. and Diallo, S. (2026) Application of Geospatial Tools and Hierarchical Multi-Criteria Analysis to the Study of Coastal Vulnerability to Flooding in San Pedro (South-West of the Ivory Coast). *International Journal of Geosciences*, **17**, 636-651.
https://doi.org/10.4236/ijg.2026.179030

Received: August 16, 2026
Accepted: September 8, 2026
Published: September 11, 2026

Abstract

San Pedro, a port city in south-western Côte d'Ivoire, is extremely vulnerable to flooding, coastal erosion and storm surges—adverse consequences of climate change. This study aims to analyse and map vulnerable areas along the San Pedro coastline by combining GIS, remote sensing and Hierarchical Multi-Criteria Analysis (AHP). The flood vulnerability map was constructed using seven key factors: slope, elevation, land cover and land use, population density, drainage density, rainfall and soil type. Of these factors, population density, land cover and slope are those with the greatest impact on flood vulnerability. This map reveals that 11.91 per cent of the study area has very low vulnerability, 20.94 per cent has low vulnerability, 22.97 per cent has medium vulnerability, 21.91 per cent has high vulnerability, and 22.27 per cent has very high vulnerability. The summary map of flood vulnerability shows that 44.18 per cent of the area under study has high to very high vulnerability, concentrated in low-lying central and coastal neighbourhoods. Only 11.91 per cent of the territory shows very low vulnerability to flooding. These results provide valuable information for decision-makers and local communities, contributing to the development of targeted mitigation strategies and raising awareness of areas vulnerable to flooding. This study highlights the importance of integrating geospatial technologies and multi-criteria analysis into flood risk assessment, in order to improve disaster preparedness and climate resilience.

Keywords

GIS, AHP, Flood Vulnerability, San Pedro, Côte d'Ivoire

1. Introduction

Coastal vulnerability is a global issue [1]. The effects of climate change, combined with population growth and the intensification of human activities, are continually exacerbating coastal risk [2]. This is the case in Africa, where coastal areas are becoming increasingly vulnerable under the combined effects of sea-level rise, rapid urbanisation and population growth, thereby increasing the exposure of populations, infrastructure and heritage to weather and marine hazards [3]. Recent studies have shown that socio-economic pressures on West African coastlines tend to exacerbate the risks of coastal flooding [2] [4] [5], exacerbated by societies' strong desire to settle near the sea.

Ivory Coast's coastal towns are not immune to this problem. This environmental problem is exacerbated by the effects of global warming [6], as demonstrated by the work of [7], which highlighted a critical retreat of the coastline and marked instability at the mouth of the Grand-Lahou River. The severity of these hazards was demonstrated as early as August 2007, when seismic-induced waves destroyed dozens of homes [8]. Today, this situation is greatly exacerbated by human pressure [2], with major development projects disrupting natural sediment transport [9]. Located in the south-west of Côte d'Ivoire, the town of San Pedro is in the grip of this environmental crisis [10]. Once a small fishing village near a river, the town of San Pedro has undergone developments linked to the construction of the port, which has led to changes in the shoreline [11]. Today, as a major economic hub due to its port activities [12], San Pedro faces both the risk of flooding and coastal erosion [13], threatening infrastructure and human lives. Between 1993 and 1997, the average rate of shoreline retreat stood at approximately 1.2 m/year [11]. Furthermore, the gradual degradation of vegetation cover due to urbanisation is further weakening the coastline. Beyond these physical processes, the city's rapid urban expansion has been accompanied by the gradual encroachment into naturally vulnerable areas such as low-lying lands, valleys, wetlands and exposed coastal areas, thereby increasing the population's exposure to coastal risks [14]. This transformation has significant implications for the occurrence of flooding.

Given this complexity, traditional risk assessment methods prove to be limited as they do not always incorporate all relevant factors in a spatial and multidimensional manner [15] [16]. To address this, the integrated approach combining geomatics and the Analytic Hierarchy Process (AHP) emerges as an ideal alternative, enabling the synthesis of physical, socio-economic and environmental variables [17]. This study therefore aims to apply Geographic Information Systems (GIS) and AHP to identify, map thematically and mathematically model the factors contributing to coastal flood vulnerability in the town of San Pedro, in order to produce a descriptive summary map of high-risk areas to aid local decision-making.

2. Presentation of the Study Area

The study area covers the coastline of the town of San Pedro, situated in the south-west of Côte d'Ivoire, the administrative centre of Lower Sassandra (**Figure 1**). It is situated between the longitudes and latitudes and covers an area of 61.20 km^2. The climate of the area is classified as a humid equatorial climate, characterised by four seasons: two wet seasons and two dry seasons. The high humidity observed in the region is due to the influence of the Atlantic Ocean and the monsoon winds, which bring large masses of moist air to the coast. The terrain is relatively flat with low elevations and consists of sedimentary plains not exceeding an altitude of 84 m. It is characterised by the presence of dead cliffs rising to between 20 and 65 m and overlooking narrow coastal plains [13]. In terms of hydrography, the San Pedro River is the main watercourse, whose tributaries (Palapod, Ménégbé, Kré) increase its flow rate at the mouth [18]. In addition to the river, the city comprises a lagoon (Digboué) and several lakes which feed a vast marshy area [19]. Its economy relies mainly on port operations, agriculture, fishing and the service sector. The presence of the port has encouraged the development of industrial and village-based plantations of cocoa, coffee and oil palm. These activities attract people from other regions and neighbouring countries, fueling sustained population growth which is exerting increasing anthropogenic pressure on coastal areas [20].

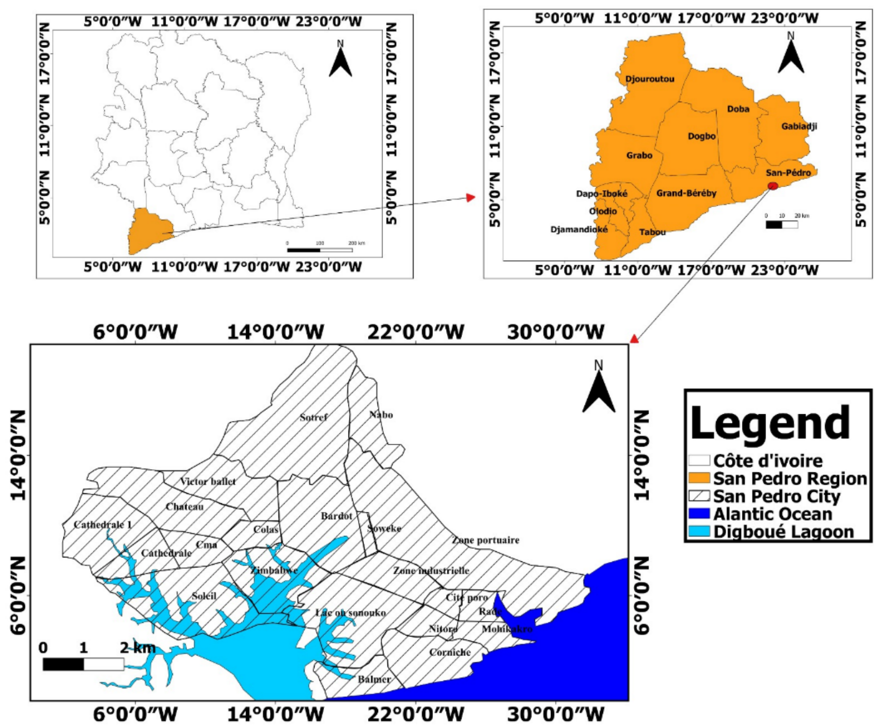

Figure 1. Location of the study area.

3. Methodology

The methodology adopted to map coastal vulnerability in San Pedro is described below.

3.1. Data Collection

The data used for this study were drawn from several complementary sources.

Satellite data include a Sentinel-2 image from 2023 for land-use mapping and SRTM data at 30-metre resolution for generating the Digital Elevation Model (DEM). Climate data were obtained from the Société d'Exploitation et de Développement Aéroportuaire, Aéronautique et Météorologique (SODEXAM) for the period 1985-2025. Demographic data were taken from the General Population and Housing Census, at the neighbourhood level in San Pedro.

3.2. Selection of Criteria

The identification of criteria is based on previous studies focusing on San Pedro. These include physical environmental constraints as well as human activities that expose the town to coastal hazards. The criteria selected are: slopes, land use, drainage density, population density, soil type, precipitation and elevation.

3.3. Mapping of Vulnerability Factors

A GIS was used to produce thematic vulnerability maps based on the criteria mentioned above. These maps represent the spatial indicators of coastal vulnerability within the study area.

3.4. Process of Weighting AHP

By applying the AHP, the research aimed to identify vulnerable areas along the San Pedro coastline. The weighting process involves comparing each criterion in pairs and assigning a weight to each one.

3.5. Vulnerability Assessment

Using thematic maps and the AHP methodology, a coastal vulnerability assessment was carried out, covering both physical and human factors in San Pedro. This section aims to select and analyse the criteria in order to identify vulnerable areas along the San Pedro coastline. The methodology utilises various datasets, remote sensing tools, GIS techniques and the AHP method to provide meaningful information on the coastal vulnerability of the study area, as shown in **Figure 2**.

3.6. Analytic Hierarchy Process (AHP)

In this study, the hierarchical multi-criteria analysis method devised by the mathematician [17] Saaty (1980) is used. AHP is a systematic technique commonly used in complex decision-making contexts, which enables difficult decision-making processes to be broken down into comprehensible elements. It follows the steps set out below.

Step 1: Define the decision-making problem

The aim is to analyse and map the coastal vulnerability of San Pedro by combining seven physical and human criteria.

Step 2: Create a hierarchy

A hierarchical structure is created, representing the main objective, the coastal vulnerability map, the seven selected criteria and the five vulnerability classes associated with each.

Step 3: Pairwise comparisons

The criteria are compared in pairs using value scale [17]. Decision-makers assess the elements on a scale of 1 to 9, where 1 represents equal importance between two elements and 9 represents the absolute importance of one element over another.

Step 4: Calculating weights

The weights of the criteria and sub-criteria are calculated on the basis of the pairwise comparisons. These weights represent the relative importance of each element within the hierarchy. The weighting coefficient (Cp) is calculated as follows:

$$\mathrm{Cp} = \frac{vp}{\sum V_p} \quad (1)$$

$\sum V_p$ is the sum of all eigenvectors. The sum of the Cp values must equal 1. Table 1 presents the value scale used for the pairwise comparisons.

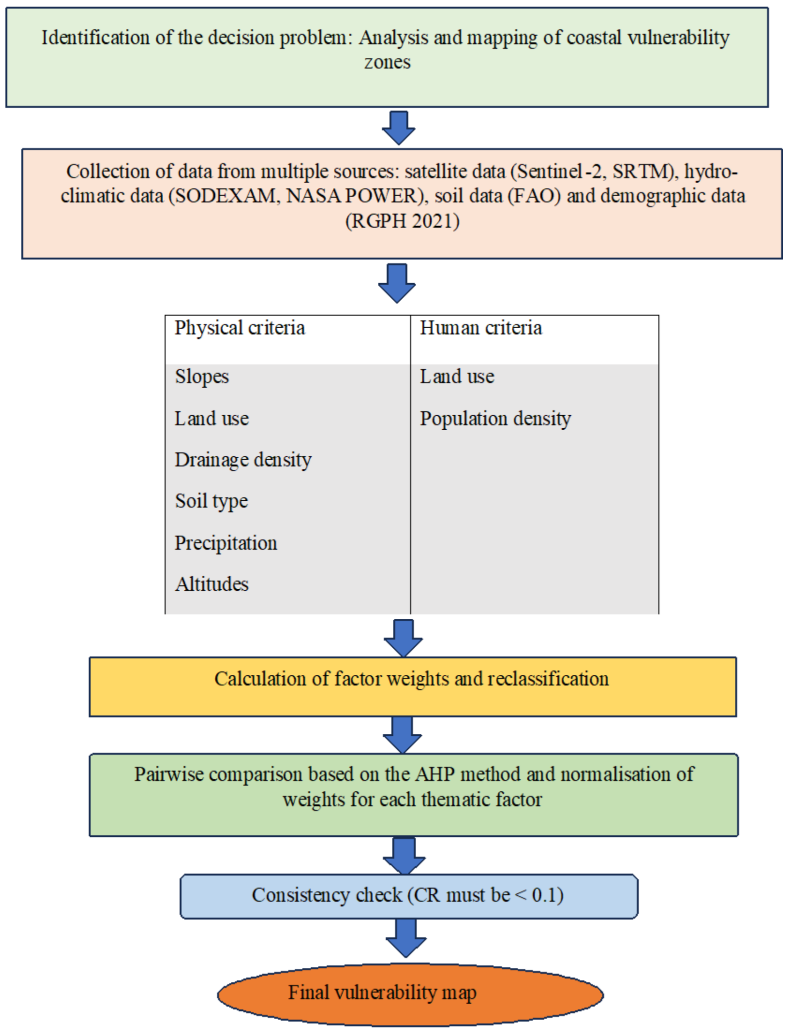

Figure 2. Flowchart of methodology.

Table 1. Saaty's value scale.

Degree of importance	Definition	Explanation
1	Equal importance of two Elements	Two elements contribute equally to the property
3	Low importance of one element compared to the other	Experience and personal judgement Slightly favour one factor over another
5	A strong or decisive importance of one element over another	Experience and personal judgement Strongly favour one element over another
7	Proven importance of one element over another	An element is strongly favoured and its dominance is demonstrated in practice
9	Absolute importance of one element relative to another	The evidence favouring one element over another is as convincing as it can be
2, 4, 6, 8	Intermediate values between two neighbouring ratings	A compromise is needed between two ratings

Step 5: Checking consistency

The consistency index is used to check whether the judgements are logical, *i.e.*, whether the pairwise comparisons are reliable and do not contradict one another. A widely used measure is the consistency ratio (CR). If the CR exceeds a certain threshold (usually 0.1 or 10%), the judgements may need to be reviewed. The formulas are as follows:

$$\mathrm{Rc} = \frac{\mathrm{Ic}}{\mathrm{Ia}} \tag{2}$$

$$\mathrm{Ic} = \frac{\lambda_{max} - k}{k - 1} \tag{3}$$

where λ_{max} is the largest eigenvalue of the pairwise comparison matrix, k is the number of criteria and Ia is the random consistency index. Table 2 shows the values of Ia as a function of the number of criteria.

Table 2. Values of the random consistency index (Ia) [17].

Number of criteria	1	2	3	4	5	6	7	8	9	10	11
Ia	0	0	1.51	0.58	0.90	1.24	1.32	1.41	1.45	1.49	1.51

Step 6: Aggregation and vulnerability assessment

Aggregation involves combining the criterion weights with the vulnerability scores for each thematic layer to produce the composite coastal vulnerability map.

Step 7: Developing the coastal vulnerability map

The criterion weights are used to create the final coastal vulnerability map, which assists managers and decision-makers in their coastal risk planning and management processes.

4. Results and Discussion

The combination of GIS tools and the AHP was successfully implemented in the town of San Pedro. This study conducted a detailed analysis of seven coastal vulnerability criteria, namely, slopes, land use, drainage density, population density, soil types, precipitation and elevations. These criteria were rigorously assessed to produce a comprehensive coastal vulnerability map that provides meaningful information on the town's level of exposure to coastal hazards. This is an interdisciplinary approach that perfectly illustrates the use of GIS and multi-criteria decision-making to solve complex problems such as coastal vulnerability, and which represents one of many modern research approaches.

4.1. Slope

Slope is essential for mapping flood vulnerability [21] [22] as it determines the trajectory and velocity of water. It is slope that transforms rainfall into rapid runoff on slopes or into dangerous stagnation in low-lying areas [23]. Areas with a gentle slope, typically found in low-lying floodplains, are more susceptible to flooding and are therefore assigned higher scores, whilst steeper slopes are less prone to flooding and receive lower scores.

Slope is classified into five categories using a reclassification tool (**Figure 3**).

The "very gentle" class corresponds to a gradient of between 0˚ and 5˚, whilst the "very steep" class extends to over 30˚. Gradient is a key factor in understanding the direction of water flow from upstream to downstream areas [24].

4.2. Land Cover and Land Use

The identification of vulnerable areas takes into account factors such as land cover and land use. Land cover and land use are essential for understanding the interactions between human activities and the natural environment. Rainwater runoff is increased when it falls on impervious surfaces such as residential areas and roads, whilst bare fields can lead to soil erosion and significant downstream runoff. Conversely, areas with dense vegetation pose fewer risks, as dense vegetation promotes the infiltration of rainwater into the soil, thereby reducing the impact of flooding compared with open land. The study area comprises various types of land cover, such as forest, cropland, settlements, bare ground and water bodies. **Figure 3** shows the land-use map of the area, which is divided into five classes. Land-use and land-cover patterns have a significant influence on the frequency of flooding; urbanised and developed areas generate persistent runoff that takes time to dissipate, making them more vulnerable to flooding than areas with bare soil or vegetation cover. The "settlement" class is the most dominant, covering 27.61 km^2, or 51.05 per cent of the total area. This is followed by "crops", which cover 15.36 km^2 (28.40 per cent). Forest accounts for 8.31 per cent of the study area (4.49 km^2). The "water" and "bare soil" classes account for 6.73 per cent (3.64 km^2) and 5.51 per cent (2.98 km^2) respectively.

4.3. Precipitation

Precipitation is a key factor that contributes significantly to flood vulnerability. Floods occur when increased surface runoff, caused by heavy rainfall, exceeds the capacity of watercourses to discharge the excess water [25].

Precipitation in the study area is unevenly distributed (**Figure 3**). Average annual precipitation in the town of San Pedro ranges from 1774.66 to 1812.57 mm and is categorised into five classes. Precipitation is classified as very low (1774.66 - 1787.84 mm), low (1787.84 - 1792.95 mm), average (1792.95 - 1797.79 mm), high (1797.79 - 1802.62 mm) and very high (1802.62 - 1812.57 mm). The areas with the highest rainfall levels exhibit the greatest vulnerabilities. Areas with very low vulnerability are those where rainfall is very low and include the districts of Corniche, Nitoro, Mohikakro and Rade. Areas of low vulnerability include Balmer, Lac Sonouko and Soweke. Areas of medium vulnerability include Zimbabwe, Bardot and part of Sotref. Areas of high vulnerability include the Colas neighbourhood, part of Sotref, Victor Ballet and Soleil. Areas of very high vulnerability are located in the north-west of the study area.

4.4. Altitudes

The figure shows the map of reclassified elevations for the study area (**Figure 3**). Higher elevations are less vulnerable, whilst lower elevations are more vulnerable to flooding. Elevations in the study area are divided into five classes: very low (5 - 17 m), low (17 - 38 m), medium (38 - 60 m), high (60 - 81 m) and very high (81 - 103 m). The town of San Pedro is thus characterised by a relatively flat terrain with low elevations. Areas of very low vulnerability cover 0.18 per cent, or 0.10 km^2, and are located in Mohikakro and Rade. Areas of low vulnerability cover 2.83 per cent, or 0.47 km^2, and are located in Mohikakro. Areas of medium vulnerability cover 0.87 per cent, or 1.53 km^2, and include Cathedral 1 and Victor Ballet. Areas of high vulnerability cover 21 per cent of the study area, or 11.37 km^2, and are located near the cathedral. Areas of very high vulnerability account for 75.12 per cent, or 40.66 km^2, and include the neighbourhoods of Colas, Soweke, Bardot, Zimbabwe Lac Sonouko and Nabo.

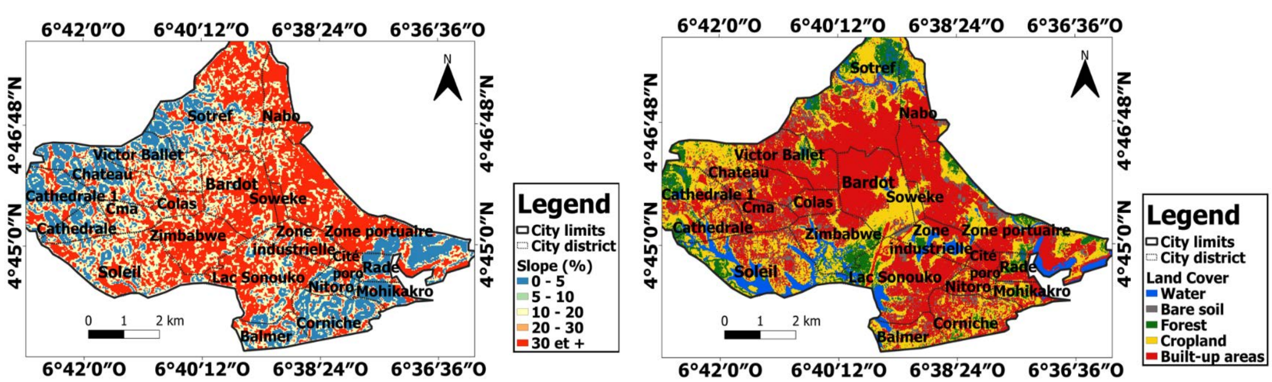

(a) (b)

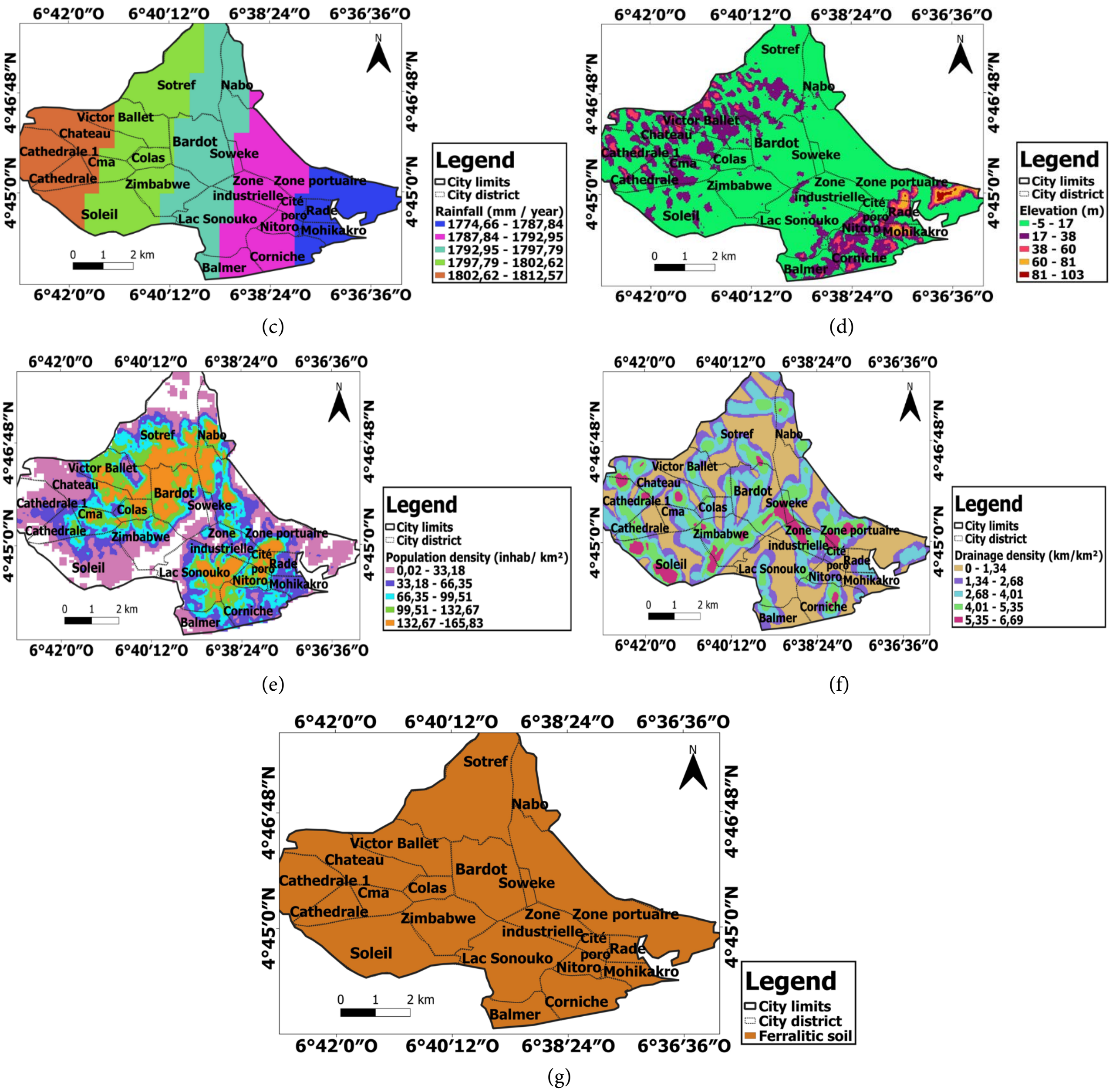

Figure 3. Spatial distribution of the flood-vulnerability factors used in the analysis: (a) Slope, (b) LULC, (c) Rainfall, (d) Elevation, (e) Drainage density, (f) Population density and (g) Soil types.

4.5. Drainage Density

The density of the drainage network is a key Hydromorphological parameter for modelling and mapping coastal vulnerability to flooding. The establishment and evolution of a drainage network depend on multiple physical variables, notably topography, the lithology of the substrate (permeability and porosity), and the configuration of local and regional fracture systems. Areas with low soil permeability tend to have high drainage density, leading to increased runoff of precipitation, and vice versa [26]. The drainage density map of the town of San Pedro, as shown in the **Figure 3**, is classified into five categories: very low (0 - 1.34 km/km^2), low density (1.34 - 2.68 km/km^2), medium density (2.68 - 4.01 km/km^2), high (4.01 - 5.35 km/km^2) and very high (5.35 - 6.69 km/km^2). The town of San Pedro is predominantly characterised by areas of very low to low drainage density.

4.6. Population Density

The higher the density, the greater the number of people vulnerable to flooding, leading to more significant socio-economic losses, including damage to infrastructure, businesses and homes. Urban sprawl destroys wetlands, forests and green spaces that naturally absorb excess water. **Figure 3** shows the population density map of the town of San Pedro. Based on these values, the classification into five distinct categories is as follows: very low, low, medium, high and very high. The highest weighting, assigned a value of 5, is given to the category ranging from 132.67 to 165.83 inhabitants per km^2, which corresponds to the highest flood risk. Conversely, the category ranging from 33.18 to 66.35 inhabitants per km^2, which corresponds to the lowest flood risk, is assigned the lowest weighting.

4.7. Soil Type

Water absorption capacity varies according to soil type [27], making infiltration a key factor in storm water management. Infiltration directly regulates surface runoff during rainfall. The soil's capacity to absorb water depends primarily on its porosity, grain size, structure, aggregation and organic matter content. The soil map of the study area shown in **Figure 3** reveals a predominance of ferralitic soils. These soils are characteristic of humid tropical regions and result from intense weathering of rocks under the influence of heavy rainfall and high temperatures. They are generally deep, well-drained and exhibit low cohesion when subjected to severe water erosion.

4.8. Coastal Flood Vulnerability Map for the Town of San Pedro

The coastal vulnerability assessment map for San Pedro was created by incorporating factors contributing to flooding, such as slope, rainfall, density of the river network, population density, elevation, land use/land cover and soil type. A decision-making approach based on the Analytic Hierarchy Process (AHP) and a Geographic Information System (GIS) was employed, with weights assigned to these parameters based on expert opinion and previous studies. To assess the vulnerability of coastlines to flooding, a pairwise comparison matrix was constructed using the AHP method to evaluate the relative importance of the selected socio-economic and infrastructural indicators (**Table 3**). The matrix was then normalised by dividing each element by the sum of its column, thereby providing a consistent scale of comparison (**Table 4**). Subsequently, **Table 5** shows the weights for each indicator, which were calculated by averaging the values in each row of the normalised matrix. A consistency check was carried out by calculating the consistency ratio (CR), which was found to be 0.047, thereby confirming that the estimates fell within the acceptable consistency range (CR ≤ 0.10).

$$\lambda_{\max} = \frac{51.83}{7} = 7.372 \tag{4}$$

$$\text{Ic} = \frac{7.372 - 7}{7 - 1} = 0.062 \tag{5}$$

$$\text{Rc} = \frac{0.062}{1.32} = 0.047 \tag{6}$$

RC = 0.047 = 4.70%, so RC < 10%; therefore, the matrix is consistent.

The final weights were integrated into a GIS environment, where each parameter layer was spatially processed and reclassified. A weighted overlay analysis was then carried out to produce the flood vulnerability assessment map (**Figure 4**), classifying the study area into zones of very low vulnerability, low vulnerability, medium vulnerability, high vulnerability and very high vulnerability. The weighted overlay method standardised and combined these factors into a unified model using the equation below.

Vulnerability map = 0.145 × slope + 0.270 × land use + 0.048 × drainage density + 0.329 × population density + 0.070 × soil type + 0.028 × precipitation + 0.112 × altitude.

Analysis of **Table 6** shows that the study area includes zones classified as having very low flood vulnerability, which cover 11.91 per cent, or 6.43 km^2, and are scattered across the area, notably in Rade and to the south-west of the port area. Areas with low vulnerability account for 20.94 per cent, or 11.31 km^2, and are situated to the north of Sotref and Château, as well as in Mohikakro. Areas with medium vulnerability cover 22.97 per cent, or 12.40 km^2, and occupy part of Soleil and Château. High-vulnerability areas account for 21.91 per cent, or 11.83 km^2, and include Corniche and Cathedral 1. Very high-vulnerability areas cover 22.27 per cent, or 12.03 km^2, and include the neighbourhoods of Bardot, Colas, Victor Ballet, Citi, Lac Sonouko, Nabo and part of Sotref. The most vulnerable areas are those with the highest population density. These classifications were determined on the basis of expert assessments of the contributing factors.

Table 3. Pairwise comparison matrix of factors contributing to coastal vulnerability to flooding.

Criteria	Slope	Land use	Drainage density	Population density	Soil type	Rainfall	Altitude
Slope	1	1/3	3	1/3	3	5	2
Land use	3	1	5	1/2	5	7	3
Drainage density	1/3	1/5	1	1/5	1/3	3	1/3
Population density	3	2	5	1	5	7	3
Soil type	1/3	1/5	3	1/5	1	3	1/2
Rainfall	1/5	1/7	1/3	1/7	1/3	1	1/5
Altitude	1/2	1/3	3	1/3	2	5	1
Totals	8366	4209	20,333	2709	16,666	31	10,033

Table 4. Normalised pairwise comparison matrix of factors contributing to flood vulnerability.

Criteria	Slope	LULC	Drainage density	Population density	Soil type	Rainfall	Altitude	Total
Slope	0.120	0.079	0.148	0.123	0.18	0.161	0.199	1.01
LULC	0.360	0.238	0.245	0.185	0.30	0.226	0.299	1.853
Drainage density	0.04	0.048	0.049	0.074	0.02	0.097	0.033	0.361
Population density	0.36	0.475	0.245	0.369	0.30	0.226	0.299	2.274
Soil type	0.04	0.048	0.148	0.074	0.06	0.097	0.05	0.517
Rainfall	0.024	0.034	0.016	0.053	0.02	0.032	0.02	0.199
Altitude	0.060	0.08	0.148	0.123	0.12	0.161	0.099	0.79
Sum	1.004	1.00	1	1.00	1	1	1	7.005

Table 5. Calculation of eigenvectors and weights for each vulnerability parameter relating to the consistency of factors contributing to flood vulnerability.

Vulnerability parameter	Eigenvector	Weighting coefficient	Weight
Slope	1.389	0.145	0.145
Land use	2.593	0.270	0.270
Drainage density	0.461	0.048	0.048
Population density	3.160	0.329	0.329
Soil type	0.669	0.070	0.07
Rainfall	0.265	0.028	0.028
Altitude	1.075	0.112	0.112

Table 6. Distribution of coastal vulnerability zones in San Pedro.

Vulnerability zone	Area (km^2)	Proportion (%)	Neighbourhoods affected
Very low	6.43	11.91	Harbour, south-west port area
Low	11.31	20.94	North Sotref, Château, Mohikakro
Medium	12.40	22.97	Soleil, Château
High	11.83	21.91	Corniche, Cathedral 1
Very strong	12.03	22.27	Bardot, Colas, Victor Ballet, Lake Sonouko, Nabo, Sotref
Total	**54.00**	**100**	

In total, 44.18 per cent of San Pedro's area is classified as having high to very high vulnerability. These areas correspond to the most densely populated areas, the lowest elevations and land uses dominated by residential areas. Conversely, only 11.91 per cent of the territory is classified as having very low vulnerability, corresponding to preserved natural areas and sparsely urbanised zones. Local authorities should monitor these areas continuously, particularly during the rainy seasons, in order to prevent disasters linked to flooding and coastal inundation. The geospatial model based on the AHP method developed in this study can help policy-makers identify and prioritise high-risk areas, thereby enabling targeted interventions, optimised resource allocation and effective spatial planning. It can also facilitate the integration of flood risks into local development plans, infrastructure projects and climate change adaptation strategies.

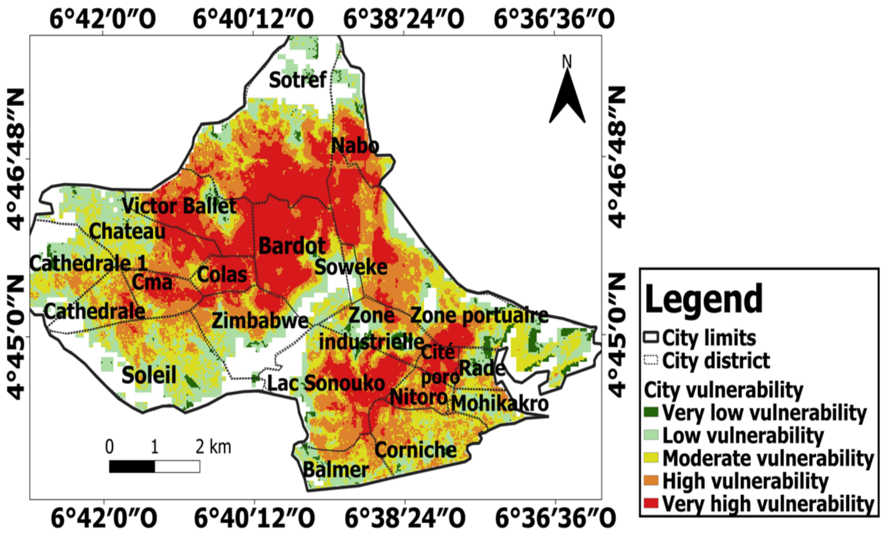

Figure 4. Flood vulnerability map of San Pedro.

5. Conclusions

The analysis of San Pedro's coastal vulnerability to flooding reveals that rainfall, slope, soil type, land use, elevation, population density and the density of the river network significantly influence vulnerability to flooding. Of these factors, population density, land use and slope are those with the greatest impact on vulnerability to flooding. San Pedro's rapid population growth and the concentration of activities in the most attractive coastal areas have led to the gradual encroachment into areas that are naturally susceptible to hazards. Urbanised and developed areas with gentle slopes, characterised by low infiltration capacity, are the most exposed to flooding. Conversely, higher-altitude areas present a lower risk of flooding. These topographical and altitudinal characteristics structurally predispose the town to the risks of flooding and coastal inundation. The fact that the drainage network is inadequate across 78.13 per cent of the municipality exacerbates the stagnation of rainwater during heavy rainfall events.

Furthermore, average annual rainfall, ranging from 1,774.66 to 1,812.57 mm, is a constant aggravating factor in these hazards. Water absorption capacity varies according to soil type, making infiltration a key factor in rainwater management. Furthermore, higher elevations are less vulnerable, whilst lower elevations are more vulnerable to flooding. More than three-quarters of the study area (75.12

per cent, or 40.66 km^2) is highly vulnerable to flooding.

The summary coastal vulnerability map reveals that 44.18 per cent of the total area of San Pedro is classified as having high to very high vulnerability. The areas of very high vulnerability, covering 22.27 per cent of the territory, include the neighbourhoods of Bardot, Colas, Victor Ballet, Lac Sonouko, Nabo and part of Sotref, which require particular vigilance and urgent preventive planning measures. Conversely, only 11.91 per cent of the territory is classified as having very low vulnerability, corresponding to preserved natural areas.

The integration of the GIS and the AHP played a key role in providing a comprehensive assessment of San Pedro's coastal vulnerability to flooding and in establishing an operational cartographic basis for urban managers, civil protection services and spatial planning decision-makers. This study makes an original contribution to our understanding of San Pedro's coastal vulnerability by producing, for the first time, an integrated multi-criteria map combining seven physical and human parameters. This study may also serve as a model for coastal cities in West Africa facing the challenges of climate change.

Acknowledgements

We would like to thank the data providers, in particular the Airport, Aeronautics and Meteorological Operations and Development Company (SODEXAM), the Côte d'Ivoire Mining Development Company (SODEMI) and the National Institute of Statistics (INS). We sincerely appreciate and thank all partners, researchers and stakeholders for their collaborative efforts.

Author Contributions

All authors (Anzoumanan Kamagate, Attoungbre Jean-Philippe Deguy and Seydou Diallo) reviewed and approved the final manuscript. Anzoumanan Kamagate wrote the protocol, collected the data, processed the data, and wrote the manuscript. Attoungbre Jean-Philippe Deguy and Seydou Diallo managed the literature research, assisted in the analysis of the data, and contributed to the interpretation of the results.

Conflicts of Interest

The authors declare no conflict of interest.

References

[1] Basnayake, V., Duong, T.M., Ranasinghe, R., Almar, R. and Wijnberg, K.M. (2026) A Global Assessment of Coastal Vulnerability and Dominant Contributors. *Nature Communications*, **17**, Article No. 578. https://doi.org/10.1038/s41467-025-67275-6

[2] Dada, O.A., Almar, R. and Morand, P. (2024) Coastal Vulnerability Assessment of the West African Coast to Flooding and Erosion. *Scientific Reports*, **14**, Article No. 890. https://doi.org/10.1038/s41598-023-48612-5

[3] IPCC (2022) Climate Change 2022: Impacts, Adaptation and Vulnerability. Contribution of Working Group II to the Sixth Assessment Report of the Intergovernmental

Panel on Climate Change. IPCC/WHO, 1-37.

[4] Alla, D.A., Atta, K.J.M and Yassi G.A (2018) Les risques naturels et leurs manifestations dans une ville secondaire: Érosion et inondation à Daloa (Centre-Ouest de la Cote d'Ivoire). *Revue de Géographie Tropicale et de l'Environnement*, **2**, 101-113.

[5] Houessinon, D.R.B., Tchibozo, E.A.M., Vissin, E.W. and Ognondoun, A. (2022) Mapping Flood Risk in the Greater Nokoué Urban Agglomeration in Benin: GIS and a Multi-Criteria Approach. *Ivorian Journal of Science and Technology*, **39**, 216-233. https://revist.net/REVIST_39/12-ST-844.pdf

[6] Adopo, K.L., Akobe, A.C., Etche, M.A., Monde, S. and AKA, K. (2014) The State of Coastal Erosion in South-Eastern Côte d'Ivoire, between Abidjan and Assinie. *Revue Ivoirienne des Sciences et Technologie*, **24**, 223-237. https://revist.net/REVIST_24/REVIST_24_15.pdf

[7] Valère, D.E.M., Fatoumata, B., Jeanne, K.M., Jean-Baptiste, K.A., Brice Hervé, M.A., Kouamé, A.K., *et al.* (2016) Cartographie de la dynamique du trait de cote a grand-lahou: utilisation de l'outil «Digital shoreline analysis system (DSAS)». *European Scientific Journal, ESJ*, **12**, 327-335. https://doi.org/10.19044/esj.2016.v12n36p327

[8] Konan, K.E., Abe, J., Aka, K., Neumeier, U., Nyssen, J. and Ozer, A. (2016) Impacts des houles exceptionnelles sur le littoral ivoirien du Golfe de Guinée. *Géomorphologie: Relief, Processus, Environnement*, **22**, 105-120. https://doi.org/10.4000/geomorphologie.11241

[9] Touré, B., Kouamé, K.F., Souleye, W., Collet, C., Affian, K., Ozer, A., *et al.* (2012) L'influence des actions anthropiques dans l'évolution historique d'un littoral sableux à forte dérive sédimentaire: La baie de Port-Bouët (Abidjan, Côte d'Ivoire). *Géomorphologie: Relief, Processus, Environnement*, **18**, 369-382. https://doi.org/10.4000/geomorphologie.9990

[10] Traore, K.M. (2016) Analysis of Vulnerabilities in the Coastal Town of San-Pedro (South-West Côte d'Ivoire). Ph.D. Thesis, Félix Hou-Phouët Boigny University, 355 p.

[11] Yao, K.S., Abe, J., Bamba, S.B., Konan, K.E. and Aka, K. (2010) Dynamique d'un périmètre littoral portuaire: La côte de San-Pédro, Sud-Ouest de la Côte d'Ivoire. *Revue Paralia*, **3**, 2.1-2.12. https://doi.org/10.5150/revue-paralia.2010.002

[12] Kouakou, N.N. (2023) Historical Review of the Evolution of Industrial Fabric in the Port City of San-Pedro and Its Surroundings (Ex-Southwestern Region). *GEOREVIEW*, **33**, 41-55. https://doi.org/10.4316/georeview.2023.02.04

[13] Diarrassouba, B., Yapi, A.C. and Kouadio, W.A. (2022) Occupation des Zones à Risques à San-Pedro (Côte d'ivoire): Entre Laxisme des Autorités et Insouciance des Populations. *European Scientific Journal, ESJ*, **18**, Article 46. https://doi.org/10.19044/esj.2022.v18n26p46

[14] Djirobo, E.C.O., Yao, B.K. and Kamagaté, A. (2024) Dynamism of the Flood Zones of the City of San Pedro (South-West of Côte d'Ivoire): Contribution of Remote Sensing and GIS. *International Journal of Agriculture & Environmental Science*, **11**, 1-12. https://doi.org/10.14445/23942568/ijaes-v11i4p101

[15] Tanim, A.H., Goharian, E. and Moradkhani, H. (2022) Integrated Socio-Environmental Vulnerability Assessment of Coastal Hazards Using Data-Driven and Multi-Criteria Analysis Approaches. *Scientific Reports*, **12**, Article No. 11625. https://doi.org/10.1038/s41598-022-15237-z

[16] Ramli, M.W.A., Alias, N.E., Yusof, H.M., Yusop, Z., Taib, S.M., Wahab, Y.F.A., *et al.* (2023) Spatial Multidimensional Vulnerability Assessment Index in Urban Area—A Case Study Selangor, Malaysia. *Progress in Disaster Science*, **20**, Article 100296.

https://doi.org/10.1016/j.pdisas.2023.100296

[17] Saaty, T.L. (1980) The Analytic Hierarchy Process. McGraw-Hill, p. 19.

[18] Morell, I. and Toilliez, J. (1974) Hydrology of San Pedro. ORSTOM Centre in Adiopudoume.

[19] Kpenou, C.J.M.P., Gbamble, B.Y.A., N'dri, K., Dally, B.M., Kouakou, L.P.M.S. and Yapi, A.J.Y. (2023) Physico-Chemical and Bacteriological Characteristics of the Waters of the San Pedro River, San Pedro, South-West Côte d'Ivoire. *Afrique Science*, **23**, 50-64. https://www.afriquescience.net/admin/post-pdfs/e44ede2ce5d49c9c87a7e50a938f6178.1718283323.pdf

[20] N'Guessan, A.A.B. and Kanga, K.V. (2024) Le développement des terminaux à conteneurs sur la Côte Ouest Africaine au prisme de la mondialisation des échanges maritimes: L'exemple de la Côte d'Ivoire. *Analele Universitatii Bucuresti: Geografie/Annals of the University of Bucharest—Geography Series*, **73**, 121-148. https://doi.org/10.5719/aub-g/73.1/6

[21] Afsari, R., Nadizadeh Shorabeh, S., Kouhnavard, M., Homaee, M. and Arsanjani, J.J. (2022) A Spatial Decision Support Approach for Flood Vulnerability Analysis in Urban Areas: A Case Study of Tehran. *ISPRS International Journal of Geo-Information*, **11**, Article 380. https://doi.org/10.3390/ijgi11070380

[22] Aju, C.D., Achu, A.L., Prakash, P., Raicy, M.C. and Reghunath, R. (2024) An Integrated Statistical-Geospatial Approach for the Delineation of Flood-Vulnerable Sub-Basins and Identification of Suitable Areas for Flood Shelters in a Tropical River Basin, Kerala. *Geosystems and Geoenvironment*, **3**, Article 100251. https://doi.org/10.1016/j.geogeo.2024.100251

[23] Vignesh, K.S., Anandakumar, I., Ranjan, R. and Borah, D. (2020) Flood Vulnerability Assessment Using an Integrated Approach of Multi-Criteria Decision-Making Model and Geospatial Techniques. *Modeling Earth Systems and Environment*, **7**, 767-781. https://doi.org/10.1007/s40808-020-00997-2

[24] Thanh Son, N., Thi Thu Trang, N., Bui, X.T. and Thi Da, C. (2022) Remote Sensing and GIS for Urbanization and Flood Risk Assessment in Phnom Penh, Cambodia. *Geocarto International*, **37**, 6625-6642. https://doi.org/10.1080/10106049.2021.1941307

[25] Tabari, H. (2020) Climate Change Impact on Flood and Extreme Precipitation Increases with Water Availability. *Scientific Reports*, **10**, Article No. 13768. https://doi.org/10.1038/s41598-020-70816-2

[26] Ashokraj, C. and Vaani, N. (2026) Geospatial and Machine Learning-Based Flood Susceptibility Assessment in Nagaon District, Assam, India. *Geocarto International*, **41**, 1-20. https://doi.org/10.1080/10106049.2026.2677319

[27] Raimbault, G., Andrieu, H., Berthier, E., Joannis, C. and Legret, M. (2002) Rainwater Infiltration through Urban Surfaces: From Impermeable Pavements to Reservoir Structures. *Bulletin des Laboratoires des Ponts et Chaussées*, No. 238, 39-50. https://hal.science/hal-05140645v1